Influence of Al and Ni Concentration on the Martensitic Transformation in Cu-Al-Ni Shape-Memory Alloys

V. RECARTE, R.B. PÉREZ-SÁEZ, E.H. BOCANEGRA, M.L. NÓ, and J. SAN JUAN

The martensitic transformation temperatures and the types of martensitic phases have been determined in a wide concentration range of technological interest for Cu-Al-Ni shape-memory alloys (SMAs) A stability diagram of martensitic phases as a function of alloy concentration has been determined. It is found that when the aluminum content increases, the transformation changes from $\beta_3 \Rightarrow \beta'_3$ to $\beta_3 \Rightarrow \gamma'_3$, with an intermediate concentration range where both martensites coexist due to a $\beta_3 \Rightarrow \gamma'_3 + \beta'_3$ transformation. On the other hand, an increase of nickel content stabilizes the martensite β'_3, changing from a mixed $\beta_3 \Rightarrow \gamma'_3 + \beta'_3$ to a single $\beta_3 \Rightarrow \beta'_3$ transformation. Furthermore, linear relationships between M_s and Al and Ni concentrations have been obtained for all types of martensitic phases.

I. INTRODUCTION

AMONG the shape-memory alloys (SMAs), the Cu-Al-Ni family is being considered as a potential industrial alloy,[1] and it represents an alternative to the classically used Cu-Zn-Al and Ti-Ni alloys. The major strength of these alloys from a technological point of view is their possible use at temperatures near 200 °C,[2] and, in this respect, they outperform the Cu-Zn-Al and Ti-Ni alloys, where the maximum phase-transition temperatures (PTTs) are limited to 100 °C[2] for several reasons.

Unfortunately, in spite of the good thermomechanical properties exhibited by the Cu-Al-Ni single crystals,[3] this family of alloys has to overcome some problems in order to fulfill the requirements of industrial applications.[1] The main technological problem comes from the brittleness of polycrystalline alloys obtained by conventional processing methods. Nevertheless, it seems that these problems could be overcome by using new powder-metallurgy processing routes.[4,5] These recent results open new challenges for the industrial applications of Cu-Al-Ni SMAs, and, consequently, a new study to solve the different technological problems of these alloys should be approached. In particular, the martensitic transformation (MT) in a commercial SMA must be highly reproducible in order to fulfill the reliability requirements imposed by technological applications. Therefore, a basic point is to control the MT temperatures and the type of martensite appearing, because this determines the hysteresis and the thermomechanical properties of the SMA. Considering that the MT temperatures are extremely sensitive to concentration changes and it is difficulty to control with high precision the concentration in ternary or quaternary alloys, it is evident that the alloy composition is the most important factor determining the MT temperatures. It is well known that PTTs, moreover, depend on other parameters such as grain size and ordering, but these are not as important as the alloy composition. It must be also taken into account that the kind of martensite obtained depends on the degree of order of the intermetallic alloy,[6] which also depends on the alloy concentration.[7]

The aim of this work is to determine the influence of the Al and Ni concentrations on the MT temperatures as well as on the type of martensitic phase in a broad range of concentrations in Cu-Al-Ni alloys. It is very useful, from a methodological point of view, to establish the influence of concentration on the MT temperatures in a well-known microstructural state that can be used as a reference. As it has been traditionally considered, in this work the reference state is the single crystal. In particular, we have studied single crystals grown by the Czochralski–Stepanov method, which, in the as-grown state and after annealing, contain a low dislocation density.[8] It allows us to compare our results with previous work and, thus, the entire concentration range of technological interest is covered.

II. PREVIOUS RESULTS

The thermally induced martensitic phases in a Cu-Al-Ni alloys can be β'_3 (18R) or γ'_3 (2H), depending on the composition. Historically, the β and martensite phases were labeled with the subindex 1, which is linked to an order at the next-nearest neighbors $D0_3$, but it should be remarked that the order of these alloys is the $L2_1$ and, consequently, according to the martensite nomenclature, we use the subindex 3 to name the β phase and the corresponding martensites.[9] In fact, martensite evolves from β'_3 to γ'_3 with increasing aluminum concentration,[10,11,12] and there is a concentration range where both kinds of martensite coexist. On the other hand, both kinds of martensite show different transformation characteristics. Their hysteresis temperatures differ by approximately 20 °C, giving rise to different transformation temperatures when both kinds of martensite coexist. The coexistence of thermally induced β'_3 and γ'_3 martensites has been observed for different concentrations and thermal treatments.[13–17] Furthermore, the volume fraction of γ'_3 martensite with respect to the β'_3 martensite increases with aging time at low temperatures[6,13,16,18] and with decreasing quenching rate.[17]

V. RECARTE, Lecturer in Physics, is with the Dpto. Física, Universidad Publica de Navarra, Campus de Arrosadia, 31006 Pamplona, Spain, R.B. PÉREZ-SÁEZ, Associate Lecturer, and J. SAN JUAN, Professor of Physical Metallurgy, Dpto. Física Materia Condensada, and E.H. BOCANEGRA, and M.L. NÓ, Professors of Applied Physics, Dpto. Física Aplicada II, are with the Universidad del País Vasco, 48080 Bilbao, Spain. Contact e-mail: wmpsanuj@lg.ehu.es

Manuscript submitted May 7, 2001.

On the other hand, due to the technological interest in the knowledge of the dependence of the transformation temperatures on the concentration, several empirical relationships have been proposed in the literature in the case of Cu-based SMAs; Reference 10 provides a review. Although there is not any particular physical reason for a linear dependence, a good agreement has been obtained using expressions like

$$M_s = A + \sum_i B_i \times \text{pct } E_i \qquad [1]$$

where M_s is the martensite start temperature, pct E_i is the concentration of the different elements, and the A and B_i are constants. It should be noted that some limitations of this simple rule of thumb have been considered by several authors.[19,20] There are several studies on the dependence of MT temperatures on concentration, but no linear relationship like Eq. [1] between M_s and concentration for the Cu-Al-Ni ternary system has been reported so far. There is experimental evidence of a linear dependence of the MT temperatures on concentration in several Cu-Al-Ni alloys, established from several studies concerning particular cases.[3,11,21–24] However, until now, there has been no systematic and quantitative study covering the entire concentration range of technological interest. Besides, although it is well known that the β'_3 and γ'_3 martensites appear in alloys with low and high aluminum contents, respectively, the influence of martensite type has not been considered when studying the influence of concentration on the MT temperatures.

Vasilenko *et al.*[11] determined the dependence of M_s on aluminum concentration for polycrystalline samples with 4 wt pct Ni. They found different dependencies for the β'_3 and γ'_3 martensites, but they did not take into account the coexistence of martensites when calculating the MT temperatures. An analogous case is found in Reference 3, where the author presents a figure from an unpublished work by K. Otsuka showing a linear dependence of the MT temperatures on concentration, but without considering the changes produced by the presence of different kinds of martensite.

Ximming *et al.*[22] studied the dependence of temperature on concentration in alloys with a constant value of 4.5 wt pct Ni and obtained a line, the slope of which diminishes at high aluminum concentration (>14.7 wt pct), because the aluminum-rich precipitates decrease the aluminum content of the matrix.[22] But, as in the works previously commented upon, they do not consider the variation of the kind of martensite in their study.

In the case of polycrystalline alloys with a 4 wt pct nickel content quenched in water at 20 °C and aged for 10 minutes at 220 °C, the following relationship between M_s and the aluminum concentration was proposed:[23]

$$M_s\ (^\circ\text{C}) = 2115 + 152 \times \text{pct Al (wt pct)} \qquad [2]$$

Yet another relationship between M_s and aluminum concentration was proposed by Mukunthan and Brown.[24] However, there is a dispersion as large as ±100 °C for M_s near room temperature, because in their review, they included results of single crystals, bicrystals, and polycrystals, which not only differ in nickel compositions (between 0 and 7 wt pct), but also in thermal treatments.

Concerning the dependence of M_s on nickel concentration, previous results[11,22] show that M_s decreases with nickel content, but the dependence seems not to be linear.

On the other hand, K. Sugimoto,[21] based on the results by Sugimoto *et al.*,[25] proposed a relationship like Eq. [1] for Cu-Al-Ni-Ti. However, in Reference 25, only five alloys were studied, and it is not possible to deduce a simple biparametric equation. Furthermore, the addition of titanium changes the MT temperatures, and the equation provided by Sugimoto cannot be extrapolated to the Cu-Al-Ni alloys.

The discrepancies between different results reported in the literature show that there is a need to compare works with the same kind of samples and also the same thermal treatments in order to remove other factors that affect the transformation temperatures (degree of order, grain size, defects, internal stresses, and precipitation). Then, in spite of the numerous works carried out on Cu-Al-Ni SMAs it looks very interesting to study the dependence of MT temperatures on aluminum and nickel composition, using samples with the same thermal treatment and examined with the same experimental techniques and taking into account the influence of the different types of martensite.

III. EXPERIMENTAL PROCEDURES

In this work, the dependence of MT on concentration in Cu-Al-Ni SMAs has been determined for single crystals with 17 different compositions, which were represented by three sets. The first set had a constant 4.00 wt pct (3.64 at. pct) Ni concentration and varying Al content; the second one had a constant 13.70 wt pct (27.15 at. pct) Al concentration and varying Ni content; and the third one had a constant 13.20 wt pct (26.27 at. pct) Al concentration and varying Ni content. The first set of concentrations intercepts the other two, which have constant aluminum contents. This map of concentrations involves the whole zone of scientific and technological interest in the ternary Cu-Al-Ni system.[26] Table I summarizes the sample compositions determined after processing using a plasma-emission spectrometer.

Transformation cycles have been obtained by means of a Perkin–Elmer DSC7 differential scanning calorimeter (DSC). The MT is a first-order transformation, the forward transformation (β phase $\Rightarrow$ martensite) being exothermic and the reverse one (martensite $\Rightarrow$ β phase) being endothermic. In addition, the amount of transformed mass is proportional to the entropy increment.[27] Therefore, the transformed volume fraction ($x(T)$) can be calculated using the following equation:

$$x(T) = \frac{1}{\Delta S} \int_{\text{start}}^{T} \frac{1}{T} \frac{dQ}{dt} \left| \frac{dT}{dt} \right|^{-1} dT \qquad [3]$$

where ΔS is the entropy change associated with the transformation:

$$\Delta S = \int_{\text{start}}^{\text{end}} \frac{1}{T} \frac{dQ}{dt} \left| \frac{dT}{dt} \right|^{-1} dT \qquad [4]$$

in which Q is the heat exchanged between sample and surroundings during the transformation and dT/dt is the heating-cooling rate. In this way, we can obtain the transformed volume fraction from calorimetric measurements. The characteristic transformation temperatures, M_s (martensite start) and M_f (martensite finish) for the forward transformation and A_s (austenite start) and A_f (austenite finish) for the reverse transformation, have been determined from the curve of

Table I. Weight Percent (Atomic Percent) Concentration of Al (±0.05 Wt Pct) and Ni (±0.03 Wt Pct) for the 17 Single Crystals Classified in 3 Sets: Set 1 at 4 Wt Pct of Ni Changing Al Concentration; and Sets 2 and 3 at 13.7Al and 13.2Al Wt Pct, Respectively, Changing Ni Concentration

Set 1 Compositions (4 Wt Pct Constant Ni Content)		Set 2 Compositions (13.7 Wt Pct Constant Al Content)		Set 3 Compositions (13.2 Wt Constant Al Content)	
Alloy	Al Wt Pct (At. Pct)	Alloy	Ni Wt Pct (At. Pct)	Alloy	Ni Wt Pct (At. Pct)
AK1	14.20 (27.96)	AK9	5.00 (4.54)	AK13	5.50 (5.05)
AK2	14.00 (27.65)	AK10	4.50 (4.11)	AK14	5.00 (4.57)
AK3	13.80 (27.28)	AK4	4.00 (3.64)	AK15	4.50 (4.14)
AK4	13.70 (27.15)	AK11	3.50 (3.11)	AK16	4.00 (3.66)
AK5	13.60 (26.97)	AK12	3.00 (2.73)	AK17	3.50 (3.23)
AK6	13.50 (26.80)				
AK7	13.40 (26.65)				
AK8	13.30 (26.48)				
AK16	13.20 (26.29)				

the transformed volume fraction. The starting and finishing temperatures have been taken at 2 and 98 pct of transformed volume fractions, respectively. The transformation hysteresis has been determined as the temperature difference between the forward and the reverse transformation when 50 pct of the volume was transformed. To carry out the calorimetric measurements and in order to retain the β phase, the samples were annealed at 900 °C for 20 minutes and then water quenched at 0 °C. After this thermal treatment, they were cleaned in a solution of 20 pct HNO_3 in water. Each measurement cycle is composed by a cooling-heating cycle, at 10 °C/min, in order to measure the forward transformation followed by the reverse one. The transformation temperatures were taken from the third transformation cycle once the MT temperatures had been stabilized.

The characteristic morphologies of the martensite phases have been identified by means of a Zeiss optical microscope with a heating-cooling stage (LINKAM THMSE 600), to follow the kinetics of the MT. The different morphologies and calorimetric transformation characteristics of each martensite phase allow us to determine, qualitatively and quantitatively, both kinds of martensite even when they both coexist. Additional X-ray measurements were performed to confirm these results.[10]

IV. RESULTS

In this section, the thermograms and the transformed-volume-fraction curves of the different alloys are analyzed and the MT temperatures are calculated. In order to obtain the MT temperatures, when both kinds of martensite coexist, a method based on the determination of the transformed volume fraction from the DSC thermograms has been proposed. Furthermore, the calculated temperatures allow us to propose an empirical relationship between the temperature of the forward transformation ($\beta \Rightarrow$ phase martensite) and the aluminum and nickel concentrations for the two kinds of martensite obtained.

A. *Transformation Cycles*

The thermograms and the transformed-volume-fraction curves ($x(T)$) for some alloys of sets 1 through 3 are shown in Figures 1 through 3, respectively. The exothermic peaks (negative heat flow) in the thermograms are linked to the forward transformation ($\beta \Rightarrow$ martensite), and the endothermic peaks (positive heat flow) are linked to the reverse transformation (martensite $\Rightarrow \beta$).

Analyzing the results from set 1 (Figure 1), it is clear that there is a general increase of transformation temperatures when the aluminum concentration decreases. Besides, the characteristics of the transformation cycle change with concentration. For low aluminum contents (the AK7 alloy), the transformation shows a smooth behavior and low hysteresis (≈10 °C). However, the alloy with a higher aluminum concentration (AK2) shows a jerky behavior, with several peaks in both transformations, and a higher hysteresis. The alloy with intermediate concentrations (AK4) shows a peak during the forward transformation, with a high-temperature side formed by a succession of sharp peaks and a smooth and continuous low-temperature side. However, the reverse transformation shows two peaks: a smooth low-temperature peak followed by a sharp high-temperature peak. As a consequence, two stages can be seen in the transformed-volume-fraction curve during the reverse transformation. Therefore, it is observed that there is a transition from a jerky behavior to a smooth one when the aluminum concentration decreases. There is also an intermediate region with a mixed behavior.

Regarding sets 2 and 3 (Figures 2 and 3), a decrease in the nickel content raises the transformation temperatures. In the case of set 2, there is also a change in the kind of transformation. The alloy with high nickel concentrations (AK9) shows a smooth behavior similar to the low-aluminum-content alloys of set 1, and the alloy poorer in nickel (AK12) shows a jerky behavior similar to the AK2 alloy of set 1. The alloys of set 3 show the same smooth behavior and low hysteresis (≈10 °C) for the entire range of nickel concentrations similar to the low-aluminum-content alloys of set 1 or the high-nickel-content alloys of set 2.

Therefore, from these results, we can conclude that, depending on the alloy concentration, there are three kinds of transformations.

(1) A transformation with a smooth behavior and low hysteresis (≈10 °C). These are the typical characteristics of a $\beta_3 \Rightarrow \beta'_3$ transformation. The micrograph of the AK16 alloy (Figure 4(a)) shows the zig-zag morphology of the β'_3 martensite variants. These β'_3 variants are

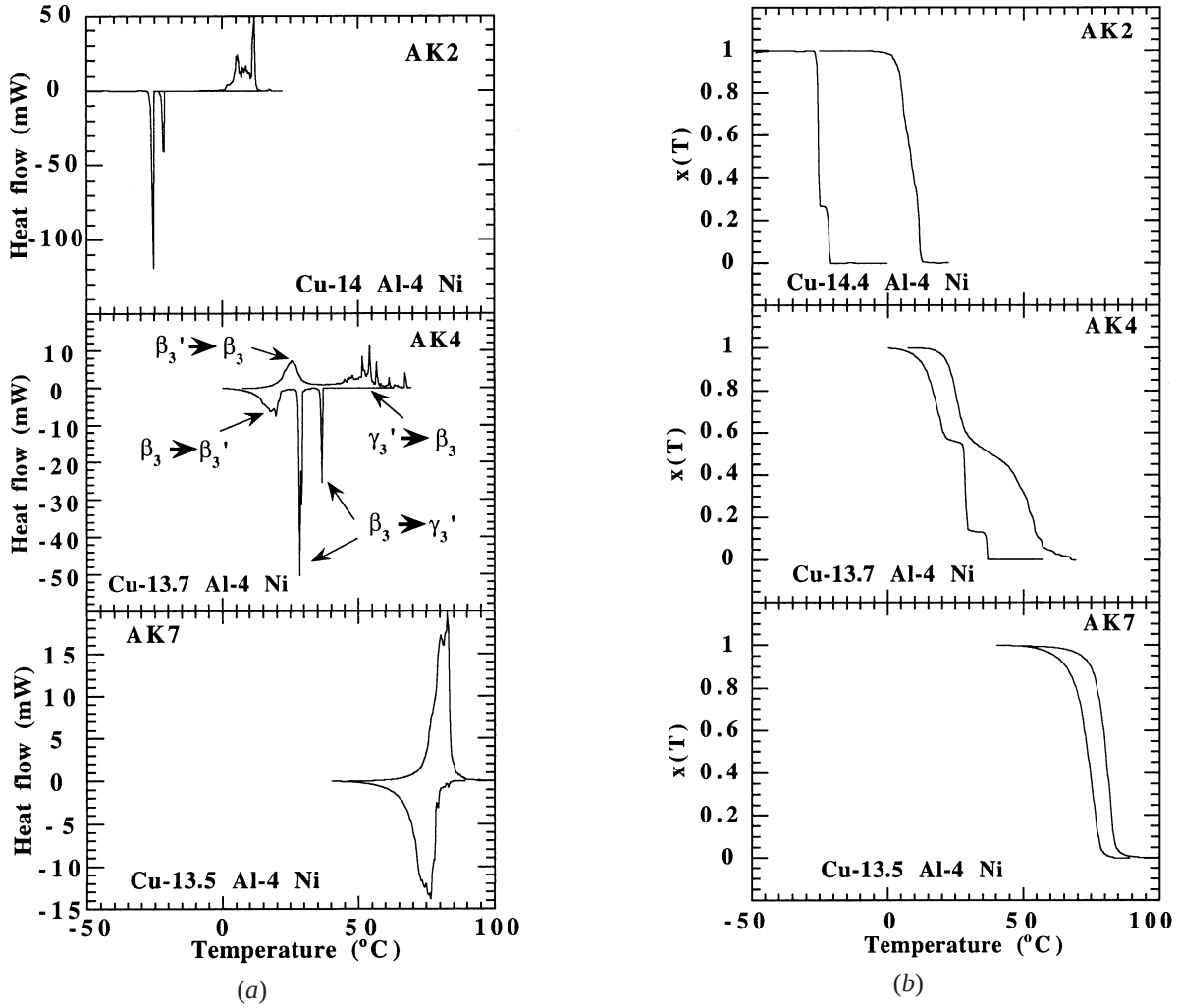

(*a*) (*b*)

Fig. 1—(*a*) Thermograms and (*b*) transformed volume fraction, $x(T)$, curves for three alloys of set 1. The thermogram of the AK4 alloy has been labeled in order to clearly indicate what peak is associated with which type of transformation.

small and have a highly thermoelastic behavior due to their controlled growth in self-accommodating groups.

(2) A jerky transformation formed by a succession of sharp peaks and high hysteresis (≈30 °C). The presence of steps in the transformed-volume-fraction curve also indicates a transformation taking place by avalanches. These are the characteristics of a $\beta_3 \Rightarrow \gamma'_3$ transformation. Big variants of γ'_3 martensite are present in the AK1 alloy (Figure 4(b)). Each sharp peak in the thermogram is linked to the sudden appearance of these variants producing a fast evolution of the transformed volume fraction and a jerky and less thermoelastic behavior.

(3) A transformation having a mixed character with two separate peaks in the reverse transformation, indicating the presence of a $\beta_3 \Rightarrow \gamma'_3 + \beta'_3$ transformation. First, big γ'_3 martensite variants appear during the forward transformation (Figure 4(c)), and later undercooling induces the β'_3 martensite variants surrounding the γ'_3 martensite variants (Figure 4(d)). Thus, the high-temperature side of the forward transformation peak is linked to the $\beta_3 \Rightarrow \gamma'_3$ transformation and the low-temperature one to the $\beta_3 \Rightarrow \beta'_3$ transformation. During the reverse transformation, there are two separate peaks due to the different hysteresis of both transformations: the low-temperature smooth peak is linked to the $\beta'_3 \Rightarrow \beta_3$ transformation, and the jerky peak at higher temperature is linked to the $\gamma'_3 \Rightarrow \beta_3$ transformation. In Figure 1(a), the thermogram of the AK4 alloy has been labeled in order to indicate what peak is associated with which type of transformation during the mixed MT.

B. *Transformation Temperatures*

The transformation temperatures have been determined from the transformed-volume-fraction curves. They are easy to obtain when there is only one transformation ($\beta_3 \Rightarrow \gamma'_3$ or $\beta_3 \Rightarrow \beta'_3$), but when there is a mixed transformation ($\beta_3 \Rightarrow \gamma'_3 + \beta'_3$), the partial transformation temperatures ($\beta_3 \Rightarrow \gamma'_3$ and $\beta_3 \Rightarrow \beta'_3$) have been obtained using a deconvolution method. Considering that the peaks of both transformations are separated during the reverse transformation, the partial transformed volume fraction of each MT ($x(\beta'_3)$ and $x(\gamma'_3)$) can be calculated (Figure 5(a)). Using these fractions, the temperatures of each transformation are determined on the total-transformed-volume-fraction curve,

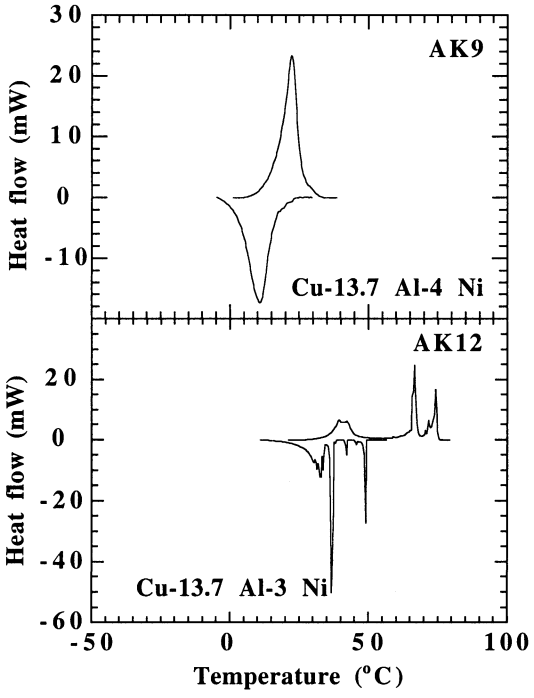

(*a*)

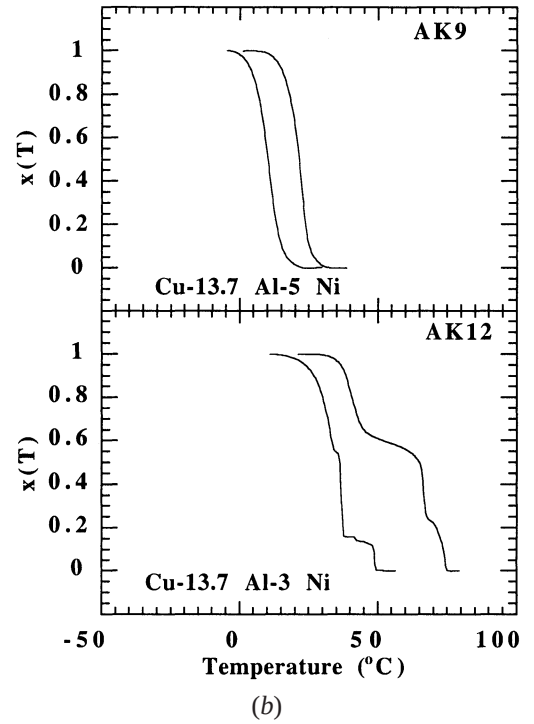

(*b*)

Fig. 2—(*a*) Thermograms and (*b*) transformed volume fraction, $x(T)$, curves for two alloys of set 2.

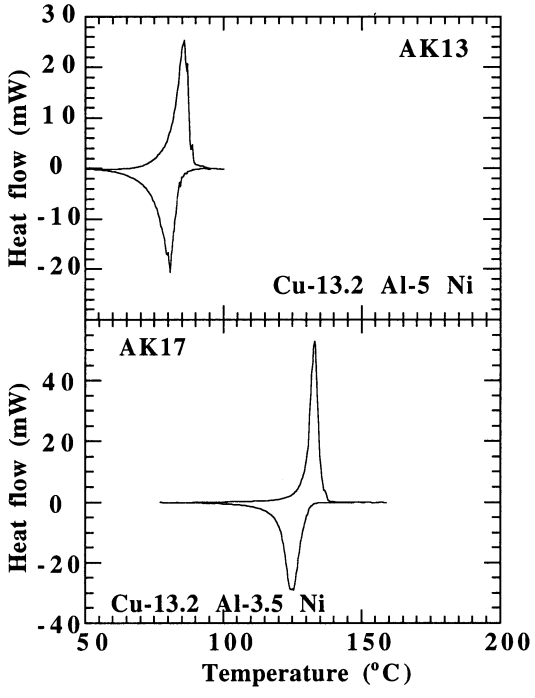

(*a*)

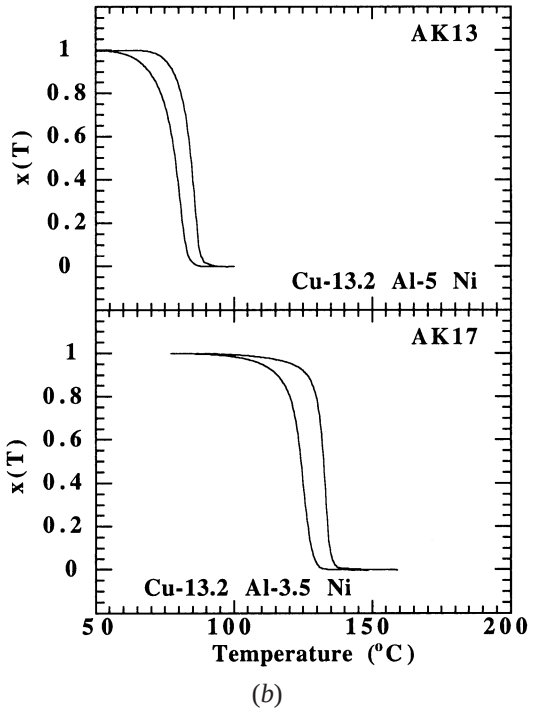

(*b*)

Fig. 3—(*a*) Thermograms and (*b*) transformed volume fraction, $x(T)$, curves for two alloys of set 3.

$X(T)$ (Figure 5(b)). For the forward transformation, we consider that both transformations take place successively, one just after the other, without taking into account any overlapping. From the point of view of the transformation temperatures, this means that $M_f(\gamma'_3) = M_s(\beta'_3)$. Actually, there could be some overlapping of both MTs, as can be deduced from the fact that loss of thermoelasticity arises during the forward transformation due to the coexistence of both martensites in a $\beta_3 \Rightarrow \gamma'_3 + \beta'_3$ MT.[28] On the other hand, the good fitting of the obtained temperatures indicates only slight overlapping and allows us to consider the proposed criterion as a good approximation.

The transformation temperatures of the 17 alloys have been obtained using the method described previously. The transformation temperatures of the alloys of set 1 are shown in Figure 6. The global transformation ($\beta_3 \Rightarrow$ martensite) M_s temperature presents a good agreement with a linear

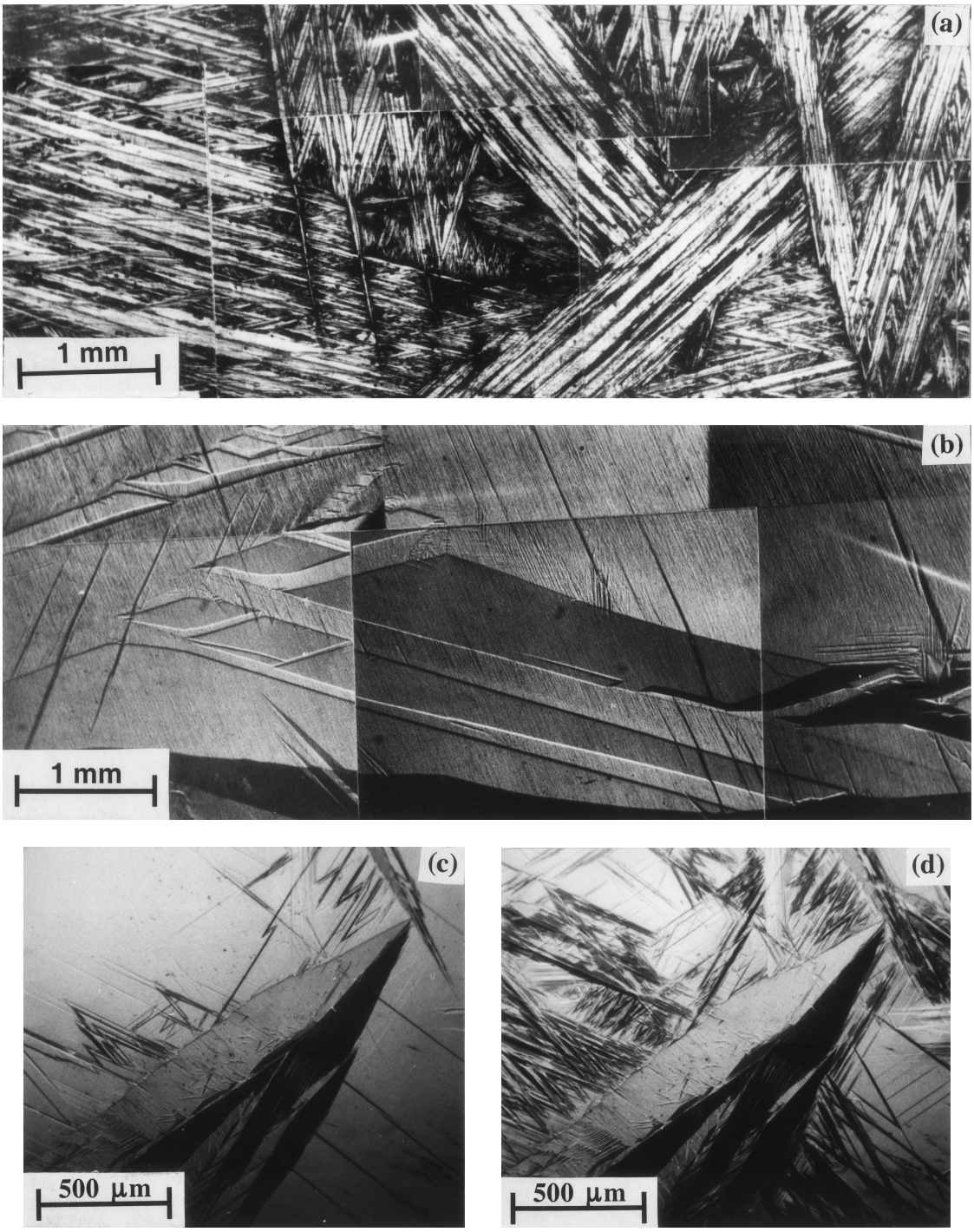

Fig. 4—Optical micrographs showing the morphology of both martensites. (*a*) β'_3 martensite variants showing their typical zig-zag self-accommodant groups in the AK16 alloy. (*b*) Big variants of γ'_3 martensite in the AK1 alloy (*c*) and (*d*) Micrograps (at −1 °C and −9 °C, respectively) of the mixed $\beta'_3 \Rightarrow \gamma'_3 + \beta'_3$ MT showing a γ'_3 big martensite variant surrounded by β'_3 martensite self-accommodant variants, in the AK3 alloy.

dependence on aluminum concentration (Figure 6(a)). Nevertheless, M_f shows an inflexion, when the aluminum concentration decreases, due to the appearance of the $\beta_3 \Rightarrow \beta'_3$ transformation, with a longer transformation interval (($M_s - M_f$), Figure 6(a)). The partial temperatures of the forward transformation obtained using the deconvolution method are shown in Figure 6(b). A slight difference of dependence on concentration and an evolution from a $\beta_3 \Rightarrow \beta'_3$ to a $\beta_3 \Rightarrow \gamma'_3$ transformation, with an intermediate region of coexistence, can be observed when the aluminum content increases. Figures 6(c) and (d) show the global reverse transformation (martensite $\Rightarrow \beta_3$) A_s and A_f temperatures and the partial ones, respectively. In general, all the transformation temperatures show a linear dependence on aluminum concentration.

The alloys of set 2 have a similar behavior, changing the kind of transformation from a single $\beta_3 \Rightarrow \beta'_3$ transformation to a mixed $\beta_3 \Rightarrow \gamma'_3 + \beta'_3$ transformation when the nickel content decreases. Thus, the forward transformation temperatures for the global transformation and for the partial transformations, after deconvolution, are shown in Figures

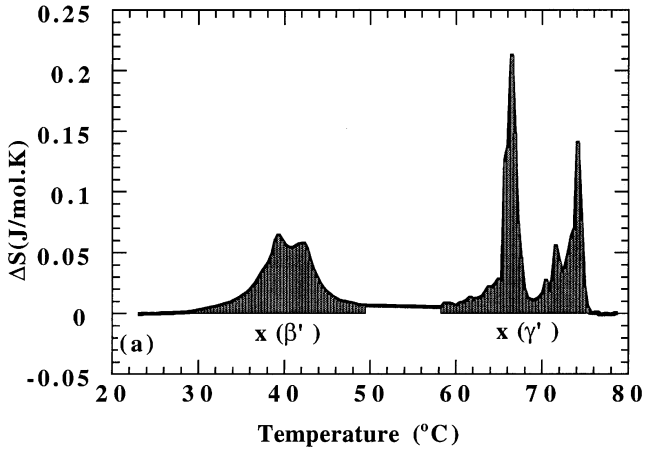

(*a*)

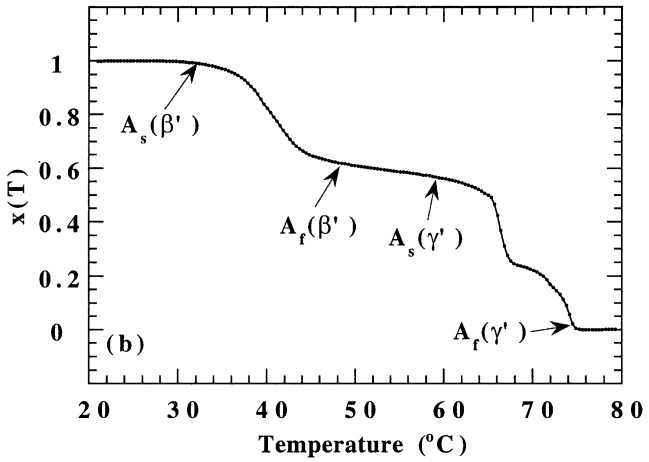

(*b*)

Fig. 5—(*a*) Entropy curve (ΔS) corresponding to the reverse transformation of a mixed MT ($\beta_3 \Rightarrow \gamma'_3 + \beta'_3$). Volume fractions of β'_3, $x(\beta')$, and γ'_3, $x(\gamma')$, martensites calculated by means of Eq. [3]. (*b*) Total transformed volume fraction curve, $X(T)$, corresponding to the reverse transformation of a mixed MT ($\beta_3 \Rightarrow \gamma'_3 + \beta'_3$). The A_s and A_f temperatures of both martensites are obtained from the corresponding volume fractions

7(a) and (b), respectively. Figures 7(c) and (d) show the corresponding temperatures for the reverse transformation. All the temperatures decrease linearly with nickel concentration. Finally, the alloys of set 3 undergo only a $\beta_3 \Rightarrow \beta'_3$ transformation; the corresponding temperatures, M_s and M_f (Figure 8(a)), as well as A_s and A_f (Figure 8(b)), decrease linearly with the nickel content.

C. *Empirical Relationship between* M_s *and the Concentration for Each Martensite*

In addition to determining the partial transformation temperatures of each martensite when the alloy undergoes a $\beta_3 \Rightarrow \gamma'_3 + \beta'_3$ transformation, the M_s temperatures calculated for each kind of martensite, γ'_3 or β'_3, have been fitted to a relationship of the type of Eq. [1]. The following results have been obtained for the γ'_3 martensite:

$$M_s\ (^\circ\text{C}) = 2280 - 157 \times \text{pct Al} - 22 \times \text{pct Ni (wt pct)} \quad [5]$$

and for the β'_3 martensite:

$$M_s\ (^\circ\text{C}) = 2660 - 187 \times \text{pct Al} - 16 \times \text{pct Ni (wt pct)} \quad [6]$$

The dependencies of M_s on composition for both martensites are similar. The temperature dependence on Al content is a bit stronger for the β'_3 martensite than for the γ'_3 martensite. On the contrary, the temperature dependence on Ni concentration is stronger for the γ'_3 martensite than for the β'_3 martensite.

D. *General Relationship between* M_s *and Concentration*

From a technological point of view, it is very important, in order to design a device, to characterize the transformation temperature *vs* concentration. Therefore, M_s has been fitted to a linear equation without considering the kind of martensite. However, we must remark that the kind of transformation changes with concentration, and this implies a different hysteresis or, even more important, a different behavior which is more or less thermoelastic. This aspect must be taken into account when designing devices. The general ($\beta_3 \Rightarrow$ martensite) M_s temperature, disregarding the kind of martensite, has been fitted to a linear equation like Eq. [1], obtaining the following result:

$$M_s\ (^\circ\text{C}) = 2433 - 169.6 \times \text{pct Al} - 19.1 \times \text{pct Ni (wt pct)} \quad [7]$$

V. DISCUSSION

In this section, the validity of the empirical relationships determined in the previous section has been tested using experimental results from the literature. Finally, the phase diagram of martensites as a function of the alloy concentration is obtained.

A. *Comparison with Previous Results*

As previously pointed out, the transformation temperature depends strongly on concentration, especially on the aluminum content. Although the concentration is the main factor controlling the transformation temperatures, there are also other microstructural, mechanical, or thermal factors which modify the transformation temperatures. Thus, depending on the thermal treatment, the state of order of the alloy can change, and so do the transformation temperatures.[6,13,17] Equally, the grain size affects the transformation temperatures, changing the elastic term of the energetic balance of the martensitic transformation.[29] These are the reasons why we are going to compare the obtained relationship only with similar samples to those used in this work, *i.e.*, single crystals quenched in water at 0 °C. Nevertheless, the dispersion shown by the experimental results extracted from literature can be attributed to several factors.

1. A different measurement technique or a different criterion for the determination of transformation temperatures is used.
2. The quenching media is the same, but the quenching rate depends on the sample size or quenching device.

The transformation temperatures obtained from the literature for alloys with nickel concentrations near 4 wt pct are

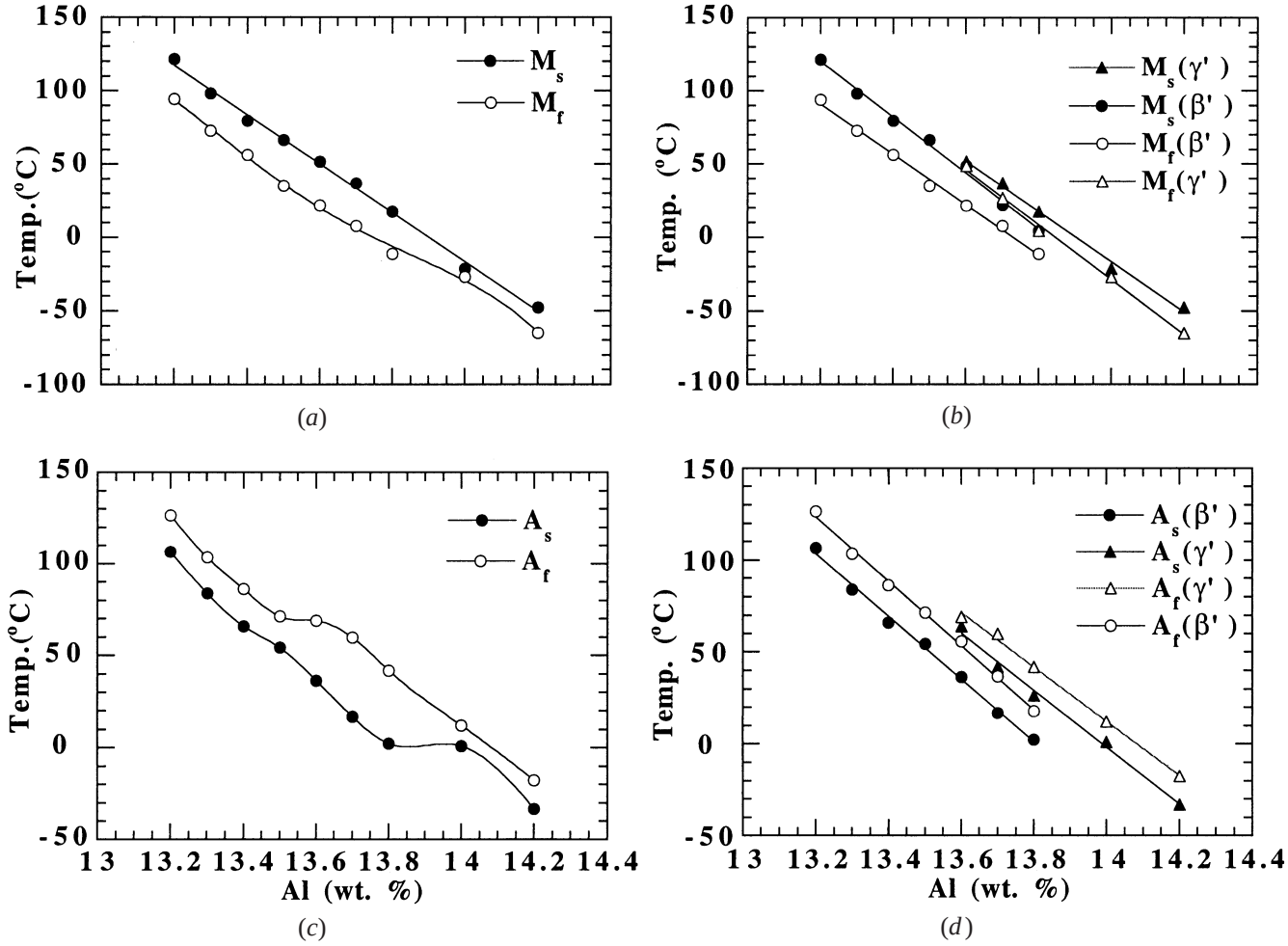

Fig. 6—Martensitic transformation temperatures of alloys of set 1. (*a*) M_s and M_f temperatures of entire forward transformation. (*b*) $M_s(\gamma'_3)$, $M_s(\beta'_3)$, $M_f(\gamma'_3)$, and $M_f(\beta'_3)$. (*c*) A_s and A_f temperatures of entire reverse transformation. (*d*) $A_s(\gamma'_3)$, $A_s(\beta'_3)$, $A_f(\gamma'_3)$, and $A_f(\beta'_3)$.

shown in Figure 9(a). Due to the weak dependence of M_s on nickel concentration, we present values at 4.2,[14] 4.1,[17] and 4 wt pct,[30] together with our results of set 1. The straight line in Figure 9(a) has been obtained from Eq. [7] for the 4 wt pct nickel. In the same way, Figure 9(b) shows the transformation temperatures at 5 wt pct nickel from Reference 11 and the alloys of sets 2 and 3, together with the line obtained from Eq. [7]. In order to check the dependence of M_s on nickel content at a constant aluminum concentration, Figure 9(c) shows four sets—14,[11] 14.1,[31] 13.7 (set 2), and 13.2 wt pct (set 3)—as well as the corresponding lines obtained from Eq. [7]. The transformation temperatures show a deviation from linearity at high aluminum concentrations for the two alloys richer in nickel. Nevertheless, sets 2 and 3, which have a lower aluminum concentration, show a linear dependence. This deviation can be linked to the presence of Al-Ni precipitates, which probably cannot be avoided for concentrations higher than 5 wt pct, even by the most severe quench. These precipitates deplete the matrix of aluminum and the transformation temperatures rise. On the other hand, a linear relationship could be too simple to be extrapolated in a wide concentration range because of the change in martensite type, but Eq. [7] seems to be valid in the range of technological interest, which is between 13 and 14.5 wt pct in aluminum and between 2 and 5 wt pct in nickel. Nevertheless, as far as the kind of martensite was known, Eq. [5] or [6] should be used.

B. *Diagram of Martensite Phases*

As has been previously pointed out, the kind of thermally induced martensite depends on alloy concentration. Taking into account the results from the literature and the present work, we have obtained the phase diagram of martensites as a function of the alloy concentration. It should be pointed out that we have only considered results from the literature for single crystals quenched in water at 0 °C, where the kind of martensite is specified.[11,14,31] Figure 10 shows the diagram of the kind of thermally induced martensite *vs* aluminum and nickel concentration, varying from 12.5 to 15 wt pct and from 0 to 6 wt pct respectively. Circles correspond to the present results, rhombuses correspond to Reference 14, squares correspond to Reference 11, and triangles correspond to Reference 31. The inverted triangles stand for the concentration limits in binary Cu-Al alloys,[32] which have been also considered to define the borderlines between the different kinds of martensite in the ternary alloys. From these results, three regions can be plotted (Figure 10), corresponding to the different kinds of thermally induced martensite, which are limited by two straight lines. The equation

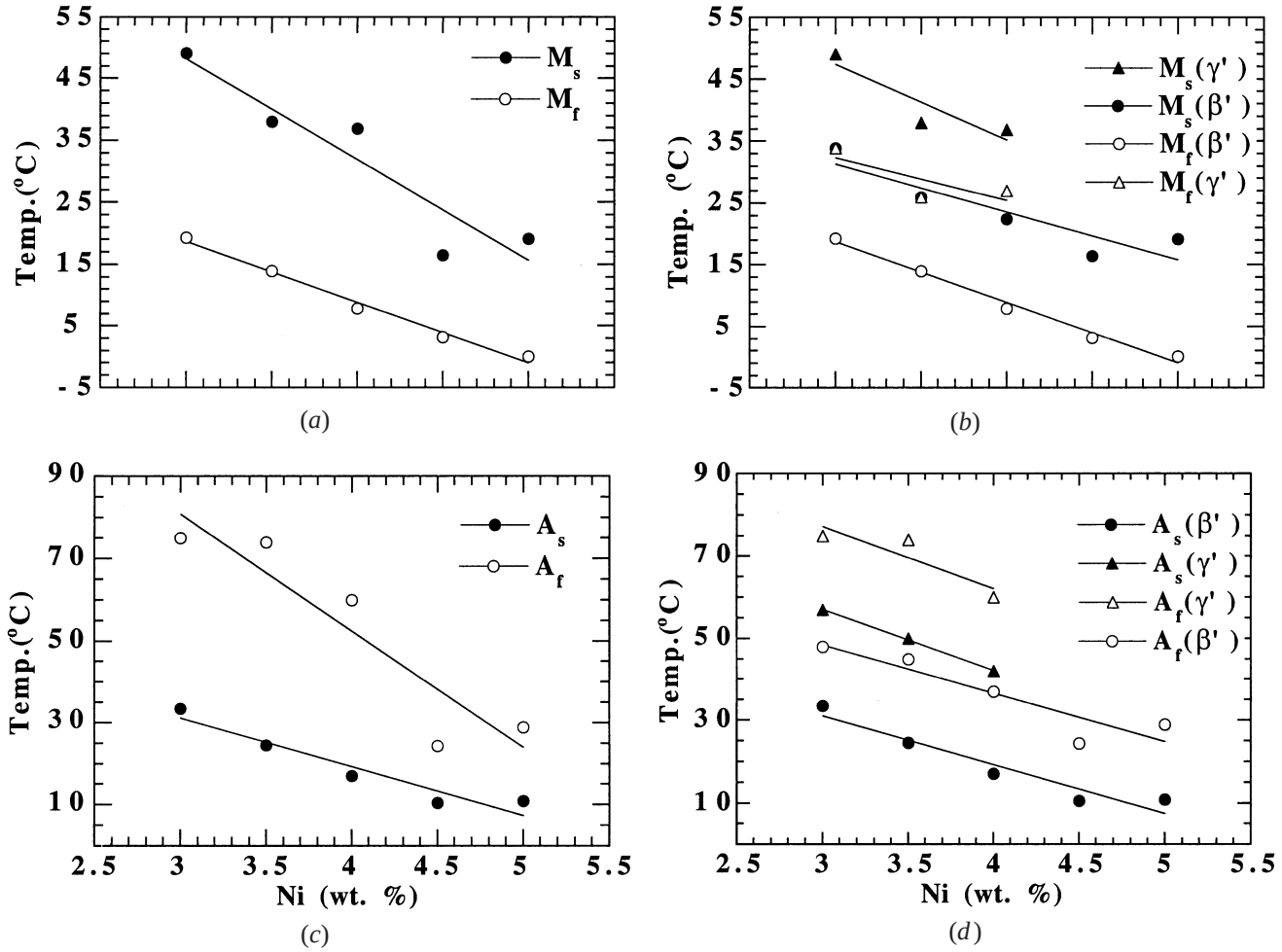

Fig. 7—Martensitic transformation temperatures of alloys of set 2. (*a*) M_s and M_f temperatures of entire forward transformation. (*b*) $M_s(\gamma'_3)$, $M_s(\beta'_3)$, $M_f(\gamma'_3)$, and $M_f(\beta'_3)$. (*c*) A_s and A_f temperatures of entire reverse transformation. (*d*) $A_s(\gamma'_3)$, $A_s(\beta'_3)$, $A_f(\gamma'_3)$, and $A_f(\beta'_3)$.

$$\text{pct Al} = 12.5 + 0.27 \times \text{pct Ni (wt pct)} \quad [8]$$

corresponds to the borderline between the β'_3 and the $\gamma'_3 + \beta'_3$ martensites, and the following one corresponds to the borderline between the $\gamma'_3 + \beta'_3$ and γ'_3 martensites:

$$\text{pct Al} = 13.15 + 0.20 \times \text{pct Ni (wt pct)} \quad [9]$$

For a low aluminum concentration, the MT is $\beta_3 \Rightarrow \beta'_3$. On the contrary, alloys with a high aluminum concentration undergo a $\beta_3 \Rightarrow \gamma'_3$ MT. Between these two regions, there is an intermediate one where a mixed $\beta_3 \Rightarrow \gamma'_3 + \beta'_3$ MT is thermally induced. Nevertheless, the increase in nickel content stabilizes the β'_3 martensite instead of the γ'_3 martensite.

On the other hand, the dashed line in Figure 10 corresponds to the eutectoid concentration of the stable-phases diagram for ternary Cu-Al-Ni alloys,[24] which is linked to the stability of the parent β_3 phase. This is an interesting point because in SMAs, the MT is only produced when the high-temperature β_3 phase is quenched at low temperature, remaining in a metastable state during the entire service life of the alloy. Consequently, further thermal aging can promote the precipitation of the stable phases by the primary precipitation of the γ_1 or α phases, followed by the eutectoid decomposition of the alloy.[10,33] So, the eutectoid line in the diagram of Figure 10 represents the concentration of highest stability of the β_3 phase and, obviously, the more stable the β_3 phase is, the more difficult the primary precipitation of the γ_1 or α phases will be. Moving away from this line implies a decrease of the β_3 phase stability and, consequently, an easier precipitation of the γ_1 or α phases. As can be seen in Figure 10, the eutectoid line is included in the region of the $\beta_3 \Rightarrow \beta'_3$ transformation. Then, alloys with these concentrations are more stable at high temperature than the alloys undergoing a $\beta_3 \Rightarrow \gamma'_3$ transformation.

Finally, the $\beta_3 \Rightarrow \beta'_3$ transformation shows the most thermoelastic character: a low hysteresis, small variants, and a progressive evolution of the transformation, as can be seen in the micrographs of Figure 4, as well as in the thermograms and integral curves of Figures 1 through 3. Thus, we can conclude that the alloys undergoing a $\beta_3 \Rightarrow \beta'_3$ transformation are the most adequate for high-temperature technological applications due to their higher thermal stability, higher degree of thermoelasticity, and, also, higher transformation temperature.

VI. CONCLUSIONS

The transformation temperatures and the kind of induced martensite in Cu-Al-Ni SMAs have been determined in a wide concentration range of technological interest. When

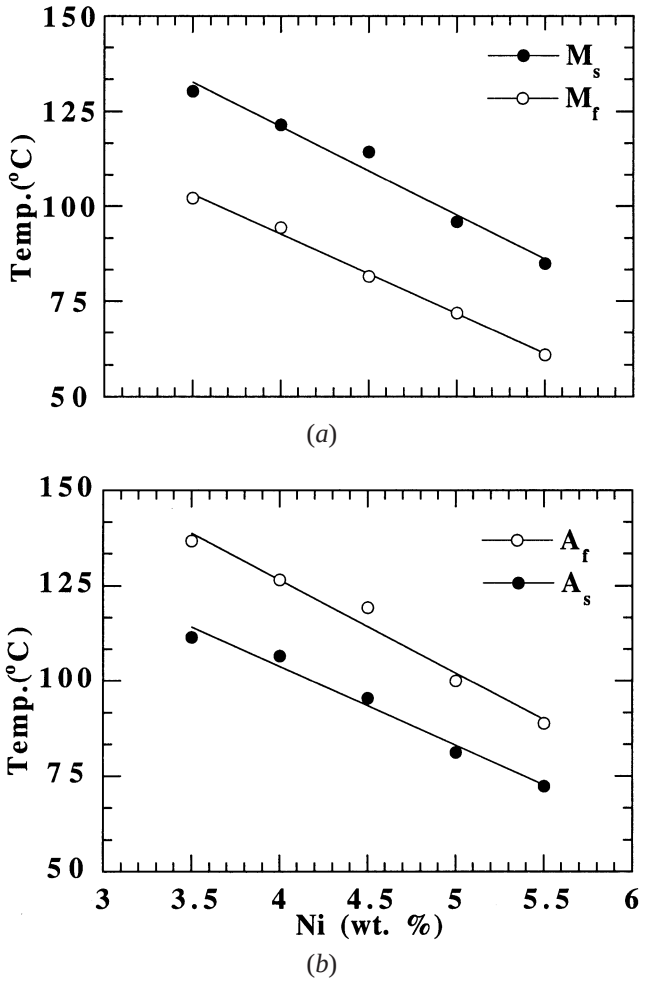

Fig. 8—Martensitic transformation temperatures of alloys of set 3. (*a*) M_s and M_f temperatures of forward transformation. (*b*) A_s and A_f temperatures of reverse transformation.

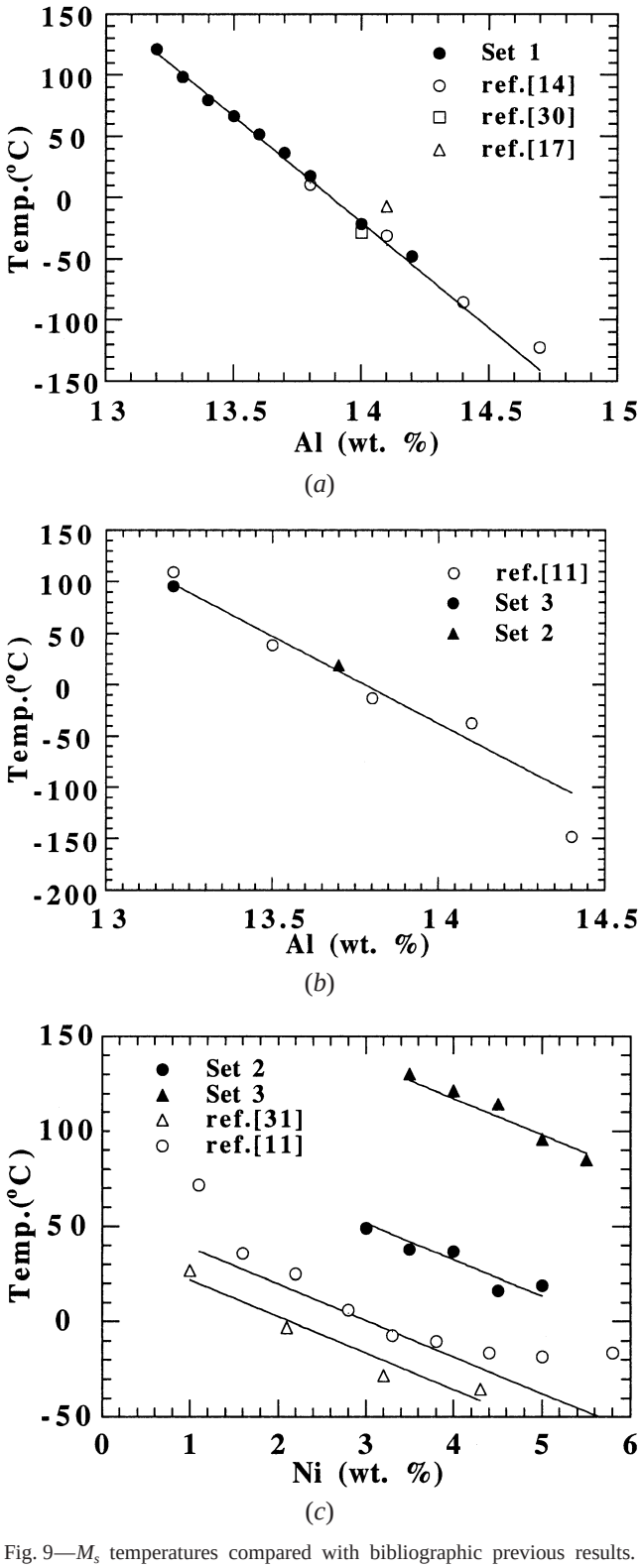

Fig. 9—M_s temperatures compared with bibliographic previous results. Lines are defined by Eq. [7]. (*a*) Alloys with nickel content near 4 wt pct. (*b*) Alloys of 5 wt pct nickel. (*c*) Four sets of alloys at a constant aluminum concentration.

the aluminum concentration increases, the MT changes from $\beta_3 \Rightarrow \beta'_3$ to $\beta_3 \Rightarrow \gamma'_3$ with an intermediate concentration range where both martensites coexist and the MT exhibits a $\beta_3 \Rightarrow \gamma'_3 + \beta'_3$ transformation. On the other hand, an increase of the nickel concentration stabilizes the martensite β'_3, changing from a mixed $\beta_3 \Rightarrow \gamma'_3 + \beta'_3$ MT to a single $\beta_3 \Rightarrow \beta'_3$ MT.

The dependence of the MT temperatures on concentration has been determined. The M_s temperature for each kind of martensite (β'_3 and γ'_3) have been fitted to a linear equation. For alloys undergoing a mixed $\beta_3 \Rightarrow \gamma'_3 + \beta'_3$ MT, a deconvolution method has been developed in order to obtain the temperatures of the partial transformations. Disregarding the kind of martensite, the global M_s temperature has been also fitted to a linear equation, which shows a strong dependence on aluminum concentration (−170 °C/wt pct) and a slight dependence on nickel concentration (−19 °C/wt pct). The obtained relationship has been compared to the bibliographic experimental results for single crystals with the same thermal treatment. The good agreement observed allows us to consider this relationship to be valid in the concentration range of interest for shape-memory applications: 1 to 6 wt pct nickel and 13 to 14.5 wt pct aluminum.

Finally, taking into account our results as well as the bibliographic results for single crystals, the diagram of the martensitic phases as a function of aluminum and nickel concentrations has been determined.

From a technological point of view, we can conclude that the results obtained in the present work constitute a powerful

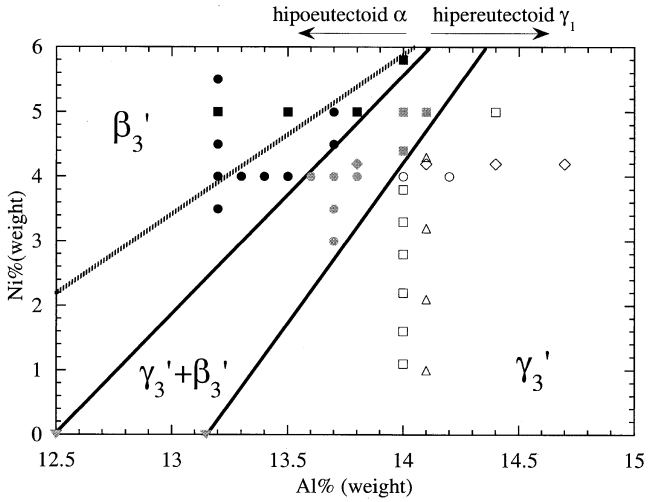

Fig. 10—Diagram of the kind of thermally induced martensite *vs* aluminum and nickel concentrations. The dashed line is the eutectoid concentration line.[24] Circles (present results), rhombuses,[14] squares,[11] triangles,[31] and inverted triangles.[32] Colors of markers: black (β'_3 martensite), gray (γ'_3 + β'_3 martensites), and white (γ'_3 martensite).

tool for the development of a Cu-Al-Ni SMA for high-temperature applications. The use of a SMA in technological applications usually necessitates, as a first step, specifying the MT temperature; alloys should be designed to fulfill this main requirement. According to the present results, a designing methodology can be proposed.

1. Once the required MT temperature has been specified, the aluminum and nickel concentration can be chosen, in a first approximation, based on Eq. [7].
2. For the different aluminum and nickel concentrations, the kind of induced martensite could be also chosen from the diagram in Figure 10.
3. According to the chosen type of martensite, the aluminum and nickel concentrations should be refined to match the specified transformation temperature, by using Eq. [5] or [6].
4. When possible, particularly for high-temperature applications, the alloys undergoing a single $\beta_3 \Rightarrow \beta'_3$ MT should be chosen, because these alloys are thermally more stable, more thermoelastic, and transform, in general, at higher temperatures.

These four criteria can be very useful for designing Cu-Al-Ni alloys and, in fact, are being successfully applied for the development of new advanced SMAs.[5]

ACKNOWLEDGMENTS

This work has been carried out with the financial support of the Spanish "Comisión Interministerial de Ciencia y Tecnología" (CICYT) in the framework of the "Plan Nacional de Materiales" (Project No. MAT 2000-1676) and the "Universidad del País Vasco" (Project Nos. UPV EB049/95 and EA127/97)

REFERENCES

1. *Shape Memory and Superelastic Technologies, Proc. SMST-94,* MIAS, Monterey, CA, 1995. Asilomar, CA, 1994, A.R. Pelton, D. Hodgson, and T.W. Duering, eds.
2. L. Delaey: in *Phase Transformation in Materials*, P. Haasen, ed., VCH, Weinheim, Germany, 1991, pp. 339-404.
3. T. Tadaki: in *Shape Memory Materials*, K. Otsuka and C.M. Wayman, eds., Cambridge University Press, Cambridge, United Kingdom, 1998, pp. 97-116.
4. J. San Juan, R.B. Pérez-Sáez, V. Recarte, I. Sáez-Ocáriz, M.L. Nó, and O.A. Ruano: *Proc. 3rd Int. Conf. on Intelligent Materials*, P.F. Gobin and J. Tatibonet, eds., SPIE Editions, Washington, DC, 1996, vol. 2779, pp. 469-74.
5. R.B. Pérez-Sáez, V. Recarte, M.L. Nó, O.A. Ruano, and J. San Juan: *Adv. Eng. Mater.*, 2000, vol. 2, pp. 49-52.
6. V. Recarte, R.B. Pérez-Sáez, M.L. Nó, and J. San Juan: *J. Mater. Res.*, 1999, vol. 14, pp. 2806-13.
7. V. Recarte, O.A. Lambri, R.B. Pérez-Sáez, M.L. Nó, and J. San Juan: *Appl. Phys. Lett.*, 1997, vol. 70, pp. 3513-15.
8. P.P. Rodriguez, J. San Juan, J.P. Morniroli, and M.L. No: *Proc. Microscopy*, Barcelona 2001, Universitat de Barcelona, Barcelona, 2001, p. 459.
9. L. Delaey and M. Chandrasekaran: *Scripta Metall. Mater.*, 1994, vol. 30, pp. 1605-10.
10. V. Recarte: Ph.D. Thesis, Universidad del País Vasco, Bilbao, Spain, 1997.
11. A.Y. Vasilenko, V.A. Sal'nikov, and A.T. Kosilov: *Phys. Met.*, 1982, vol. 4, pp. 694-701.
12. C.M. Friend: *Scripta Metall.*, 1989, vol. 23, pp. 1817-20.
13. J. Van Humbeeck, D. Van Hulle, L. Delaey, J. Ortín, C. Seguí, and V. Torra: *Mater. Trans. JIM*, 1987, vol. 28, pp. 383-91.
14. C.M. Friend, J. Ortín, A. Planes, Ll. Mañosa, and M. Yoshikawa: *Scripta Metall. Mater.*, 1990, vol. 24, pp. 1641-45.
15. V. Agafonov, P. Naudot, A. Dubertret, and B. Dubois: *Scripta Metall.*, 1988, vol. 22, pp. 489-94.
16. V. Recarte, M.L. Nó, and J. San Juan: *J. Phys. IV*, 1995, vol. 5, pp. 175-80.
17. H. Sakamoto and K. Shimizu: *Iron Steel Inst. Jpn. Int.*, 1989, vol. 29, pp. 395-404.
18. V. Recarte, R.B. Pérez-Sáez, M.L. Nó, and J. San Juan: *J. Appl Phys.*, 1999, vol. 86, pp. 5467-73.
19. M. Ahlers: *Progr. Mater. Sci.*, 1986, vol. 30, pp. 135-86.
20. N. Mwanba: Ph.D. Thesis, Katholike Universiteit Leuven, Leuven, Belgium, 1984.
21. K. Sugimoto: *Bull. Jpn. Inst. Met.*, 1985, vol. 24, pp. 45-51.
22. Z. Ximming, L. Siong, Z. Yun, M. Jialong, and N. Yuantao: *Proc. Int. Symp. on Shape Memory Alloys*, Gullin, China, 1986, pp. 261-66.
23. P. Rodriguez: Ph.D. Thesis, INSA Lyon, France, 1989.
24. K. Mukunthan and L.C. Brown: *Metall. Trans. A*, 1988, vol. 19A, pp. 2921-29.
25. K. Sugimoto, K. Kamei, H. Matsumoto, S. Komatsu, K. Akamatsu, and T. Sugimoto: *J Phys.*, 1982, vol. 43, pp. C4-761-C4-766.
26. *Ternary Alloys*, G. Petzow and G. Effenberg, eds., VCH, Weinheim, Germany, 1991, vol. 4.
27. J. Ortín, Ll, Mañosa, C.M. Friend, A. Planes, and M. Yoshikawa: *Phil. Mag. A*, 1992, vol. 65, pp. 461-75.
28. C. Seguí, E. Cesari, and J. Van Humbeeck: *Mater. Trans. JIM*, 1990, vol. 31, pp. 375-80.
29. J. Ortín and A. Planes: *Acta Metall.*, 1988, vol. 36, pp. 1873-89.
30. N. Kuwano and C.M. Wayman: *Metall. Trans. A*, 1984, vol. 15A, pp. 621-26.
31. H. Sakamoto, M. Yoshikawa, and K. Shimizu: *Mater. Trans. JIM*, 1990, vol. 31, pp. 848-54.
32. P. Duval and P. Hayman: *Mem. Sci. Rev. Métall.*, 1971, vol. LXVIII, pp. 55-63.
33. V. Recarte, I. Hurtado, J. Herreros, M.L. Nó, and J. San Juan: *Scripta Mater.*, 1996, vol. 34, pp. 255-60.